Systems & Control Transactions

Original Research Article
Peer Reviewed Conference Proceeding
ESCAPE 36 - European Symposium on Computer Aided Process Engineering
Sheffield, UK. 21-24 June 2026

PSE PRESS

A Universal Framework for Automated Reaction Network Identification and Interpretable Rate Model Generation

Harry Kay[a], Alexander Rogers[a], and Dongda Zhang[a]*

[a] The University of Manchester, Department of Chemical Engineering, Manchester, M13 9PL, UK
* Corresponding Author: dongda.zhang@manchester.ac.uk

ABSTRACT

Mathematical models are paramount to the field of reaction engineering, facilitating reaction mechanism discovery, process optimisation, and informed decision making in academic and industrial settings. Nevertheless, the development of precise mechanistic reaction rate models remains experimentally intensive, requires expert knowledge, and is susceptible to the introduction of structural bias. Similarly, the identification of a suitable reaction network that depicts all chemical transformations remains a non-trivial task, with existing techniques often being ill-suited for large and complex systems, hence limiting their scalability and implementation within chemical and biochemical applications. This work develops a two-stage autonomous framework that exploits non-linear sparse optimisation to identify the minimum size global reaction network representative of the system under study, and subsequently proposes and discriminates between interpretable rate equations developed through symbolic regression (SR). The generated SR expressions are constrained to a mechanistically meaningful form through the use of a novel substructure decomposition strategy, largely reducing the search space that must be explored and increasing model interpretability. The framework is evaluated on two case studies; the first, depicting a catalytic methanol synthesis reaction network, and the second, an enzymatic kinetic resolution network. The methodology exhibited high levels of accuracy, scalability, data efficiency, and robust network identification consistent with known physics. Lastly, the potential of augmented intelligence, is discussed as a method to enhance fidelity. Therefore, this work represents a key step toward autonomous process modelling and digitalisation in reaction engineering, providing a foundation for accelerated design and development of chemical and biochemical processes.

Keywords: Reaction network identification, Symbolic regression, Interpretable model construction, Model based design of experiments, Augmented intelligence

INTRODUCTION

The growing global emphasis on sustainability, coupled with mounting economic pressures, has driven the chemical and biochemical industries to seek more efficient processes with reduced waste, energy consumption and raw material costs. A central aspect to enabling the advancement of (bio)chemical processes is the accurate characterisation of reaction mechanisms through reliable modelling techniques, which underpins process optimisation, scale-up, and control.

Conventional modelling practices are typically based on first-principle [1-3] or empirical kinetics such as power-law, Langmuir–Hinshelwood, or Michaelis–Menten expressions [4-7] due to their ability to impart kinetic understanding through their inherent interpretability. However, for complex reaction networks that are less well understood, identifying a representative model is difficult [8], and accounting for all physical phenomena may drive model complexity beyond means which available data can sustain [9]. In order to limit complexity, expert knowledge is exploited, which introduces inductive bias and may reduce model generalisability.

In order to eliminate introducing inductive bias for reaction rate model construction, recent literature has focused on developing efficient automated chemical reaction network (CRN) identification techniques. By formulating the CRN as a mixed-integer linear programming

problem [10, 11], all mass balanced chemical transformations can be found, and rate expressions fitted to experimental data assuming first-order or categorical power law dependencies. However, if the reaction under study is defined by complex kinetics, such as typical within catalytic systems, simple power law dependencies are not sufficient for capturing the underlying physics. Additionally, for reaction networks described by larger numbers of species, the number of mass balanced models that must be evaluated increases exponentially. As a result, existing modelling approaches struggle with accuracy and scalability, particularly for complex systems which are commonplace in industrial and academic research.

To address these challenges, this work introduces a universal data-driven framework for automated reaction network identification and generation of interpretable rate expressions that resemble mechanistic models. We develop a sparse regression based optimisation strategy to effectively identify the underlying reaction network, and evolve an iterative symbolic regression (SR) procedure integrated with model-based design of experiment (MBDoE) to maximise information gain, thus facilitating rapid discovery of mechanistic knowledge for complex reaction systems. The framework was validated on two case studies: (i) a heterogeneous catalytic methanol synthesis reaction network defined by 3 complex Langmuir-Hinshelwood type rate expressions representative of an industrial reaction, and (ii) a larger kinetic resolution network defined by 9 states and 5 net reactions.

We thoroughly investigate how the different attributes of a reaction system influence the identification of characteristic and balanced reaction networks, the achievable model accuracy of any generated SR expressions, and the prospective mechanistic insight that can be gained. Finally, the prospect of augmented intelligence is examined, integrating available domain knowledge with data-driven interpretable modelling in order to accelerate the model development process and promoting the discovery of kinetic knowledge that is physically meaningful. Consequently, this study highlights the potential of the developed framework towards autonomous reaction rate modelling and discovery of process knowledge for chemical and biochemical engineering applications.

CASE STUDIES

In this work, two in-silico case studies were implemented based on real world scenarios. The first delineates the heterogeneous catalytic hydrogenation of carbon dioxide [12] to methanol and was selected due to the complex nature of the rate expressions that describe the underpinning physics. The second study is an enzyme catalysed kinetic resolution reaction network [13], which was chosen to represent a larger reaction system, hence testing the scalability of the developed framework.

Methanol Synthesis from CO_2 Hydrogenation

The first case study examines the catalytic hydrogenation of CO_2 over an unsupported In_2O_3 catalyst. Experiments were performed in an isothermal fixed-bed reactor operated under isobaric conditions, with both internal and external mass transfer limitations assumed to be negligible. A comprehensive description of the experimental configuration and the corresponding operating conditions is provided in [12]. Within the operating regions that were investigated, three reversible reactions (R1) were identified that govern the systems behaviour as follows:

$$\begin{aligned} CO_2 + 3H_2 &\rightleftharpoons CH_3OH + H_2O \;\Delta G(25°C) = -0.47kJ\ mol^{-1} \\ CO_2 + H_2 &\rightleftharpoons CO + H_2O \;\; \Delta G(25°C) = 23.4kJ\ mol^{-1} \\ CO_2 + 4H_2 &\rightleftharpoons CH_4 + 2H_2O \;\; \Delta G(25°C) = -130.8kJ\ mol^{-1} \end{aligned} \quad (R1)$$

where the first reaction corresponds to the primary methanol formation pathway via CO_2 hydrogenation, and the second and third represent competing side reactions, namely the water–gas shift and methanation reactions. To enable reaction network identification within this in-silico study, four initial experiments were generated, yielding 16 data points across 6 state variables. All generated data was simulated using the literature proposed kinetic model at a temperature of 493 K and weight hourly space velocities (WHSV) ranging from 6000 to 16000 mL g^{-1}_{cat} h^{-1}.

The kinetic expressions that describe this system are highly non-linear and have been shown characteristic of standard industrial reactions. Notably, the application of an automated rate model generation technique to a case study high kinetic complexity has not previously been reported in the literature [14]. The ground truth expressions adopted to simulate the in-silico methanol synthesis system are provided in Equation 1.

$$\begin{aligned} r_1 &= \frac{k_1(P_{CO_2}P_{H_2}^3 - \frac{P_{CH_3OH}P_{H_2O}}{K_{eq,1}})}{P_{H_2}^2\left(1 + K_{CO_2}P_{CO_2} + \sqrt{K_{H_2}P_{H_2}}\right)^2} \\ r_2 &= \frac{k_2\left(P_{CO_2}P_{H_2} - \frac{P_{CO}P_{H_2O}}{K_{eq,2}}\right)}{\sqrt{P_{H_2}}\left(1 + K_{CO_2}P_{CO_2} + \sqrt{K_{H_2}P_{H_2}}\right)^2} \\ r_3 &= \frac{k_3\sqrt{P_{CO_2}}\sqrt{P_{H_2}}(1 - \frac{P_{CH_4}P_{H_2O}^2}{K_{eq,3}P_{CO_2}P_{H_2}^4})}{\left(1 + K_{CO_2}P_{CO_2} + \sqrt{K_{H_2}P_{H_2}}\right)^2} \end{aligned} \quad (1)$$

Here, r_1, r_2 and r_3 refer to the global reaction rates for methanol synthesis via CO_2, the water gas shift, and the methanation reaction, respectively. K_j and P_j are the adsorption equilibrium constants and partial pressures of

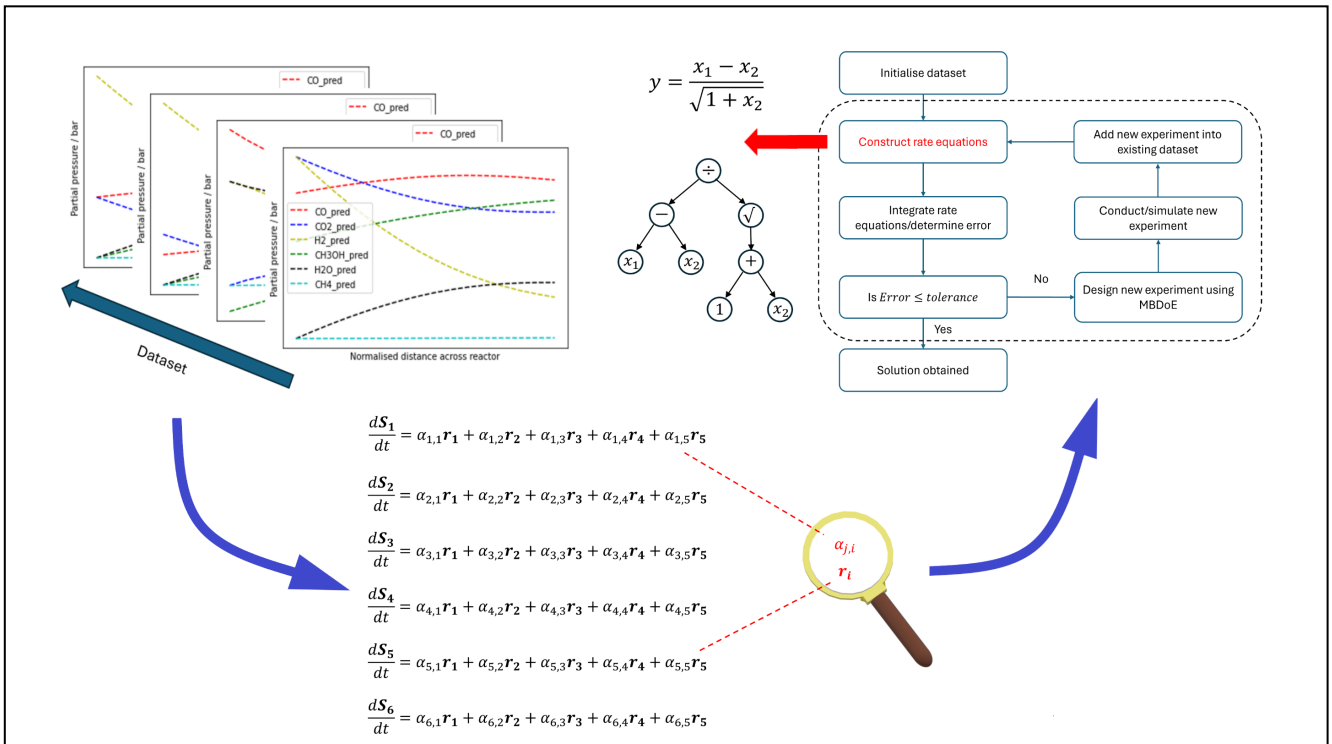

Figure 1: Schematic of the general devised framework for the identification of reaction networks and construction of representative rate equations

species j. k_i and $K_{eq,i}$ represent the reaction rate constant and equilibrium constant for a given reaction i. All values used to parameterise Equation 1 can be found in [12].

Enzyme Catalysed Kinetic Resolution

The second case study investigates the construction of kinetic models for the kinetic resolution of (+-)-trans-1, 2-cyclohexanediol in supercritical CO_2. The reactions take place in a batch reactor containing immobilised enzymes which is operated under isothermal and isobaric conditions. All developed literature rate models were formulated under the assumptions that: all reaction steps are elementary, the concentration of non-activated enzyme remains in excess, the catalysed reactions proceed irreversibly, and perfect mixing is maintained. Additional details surrounding the experimental setup and modelling assumptions can be found in [13].

For the purpose of the present study, the formation of the diacetate product S_3 was not ignored in the network to investigate the influence of minor side reactions on the accuracy of the proposed network identification and model generation framework. The reaction network and corresponding rate expressions used as the ground truth for generating the in-silico data are presented in Reaction Network (R2) and Equation (2).

$$VA \rightleftharpoons \mathrm{AE} + AA$$

$$AE + S_1 \rightarrow S_2 \tag{R2}$$

$$AE + S_2 \rightarrow S_3$$

$$AE + R_1 \rightarrow R_2$$

$$AE + R_2 \rightarrow R_3$$

$$r_1 = k_1 C_{VA} - k_{-1} C_{AE} C_{AA}$$

$$r_2 = k_2 C_{AE} C_{S_1}$$

$$r_3 = k_3 C_{AE} C_{S_2} \tag{2}$$

$$r_4 = k_4 C_{AE} C_{R_1}$$

$$r_5 = k_5 C_{AE} C_{R_2}$$

Species VA, AE and AA denote vinyl acetate, the active enzyme, and the by-product acetaldehyde, respectively. S_1 and R_1 correspond to cyclohexanediols, S_2 and R_2 to the monoacetate products, and S_3 and R_3 to the diacetate products, with R and S indicating the respective enantiomers. The terms r_i and k_i, in Equation 2, are the global reaction rate and rate constant of reaction i, while C_j denotes the concentration of species j. All parameter values used to parameterise the rate are reported in [13].

Similar to the previous case study, four in-silico experiments were generated, however since there are 9 state variables and 5 overall reactions present, more datapoints are required for network identification; consequently, 21 datapoints were collected per experiment.

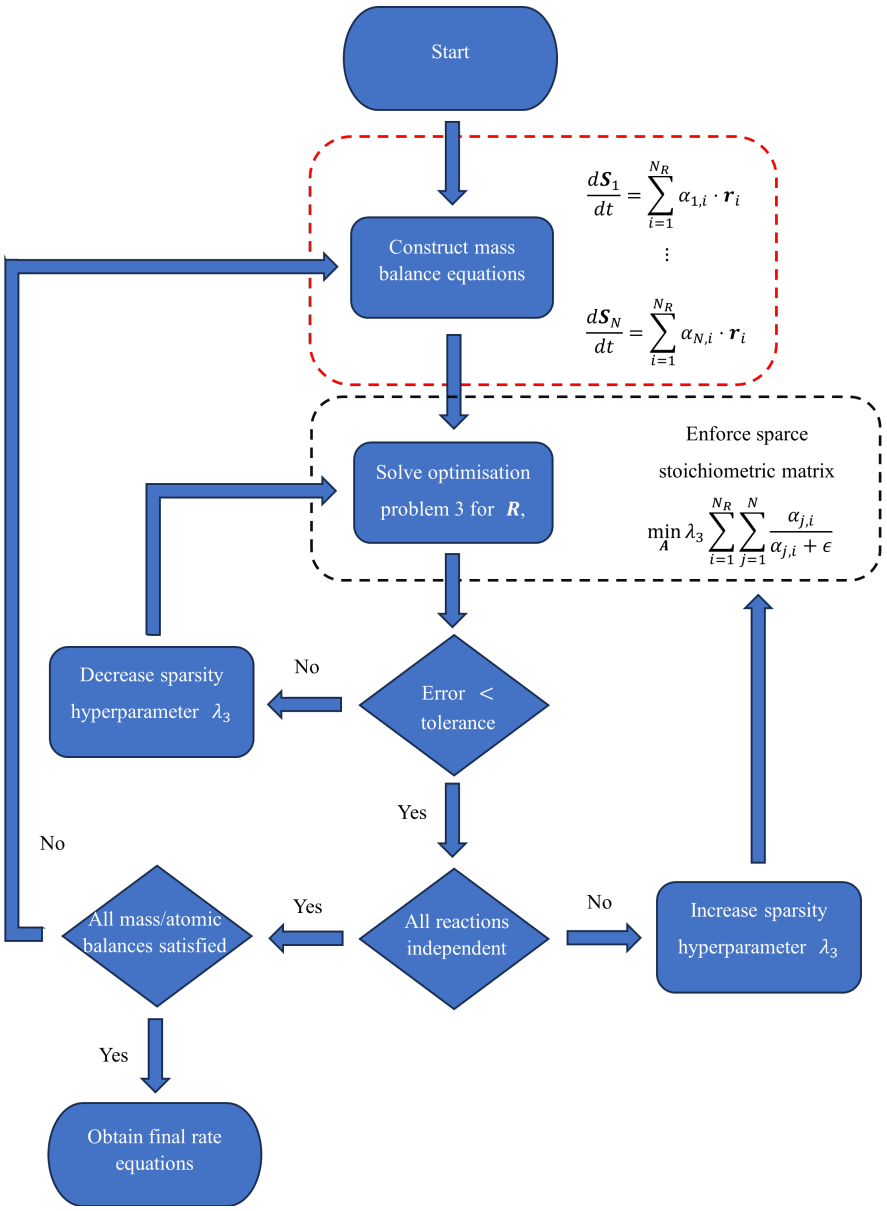

Figure 2: Flowchart representation of the methodology for identifying the minimum size global reaction network

METHODOLOGY

This section will summarise the development of the data-driven framework for autonomous reaction network identification and reaction rate model generation. Explicitly, we will first detail the method used for ascertaining the minimum number of global reactions in addition to the active species involved, then we will show the iterative symbolic regression (SR) strategy employed for the construction and refinement of representative rate equations as illustrated in Figure 1.

To reduce the associated computational expense, we propose a 2-stage workflow. Firstly, we exploit the experimental data to formulate a non-linear programming problem, subject to mass balance constraints, that yields the active reactions, their net reaction rates, $\boldsymbol{R} = \{r_1, r_2 \dots\}$, and the stoichiometric matrix, $\boldsymbol{A}$. Next SR is employed in conjunction with MBDoE in an iterative fashion to produce informative experiments that can facilitate model discrimination and improve the SR results. The iterations continue until no improvements are observed in the pareto front of proposed model candidate or until a threshold criterion is met.

Reaction Network Identification

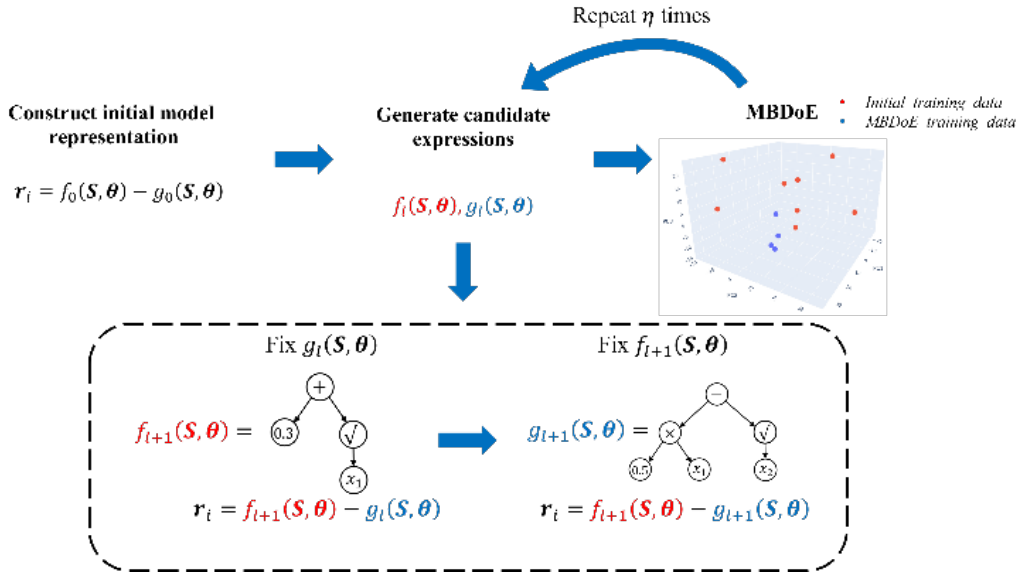

Figure 3. Diagram of the iterative approach used for generating rate expressions from data across η global iterations of the framework at local iteration, l, of tuning the SR model structure.

A chemical reaction network (CRN) is described by a set of characteristics, being the number of global reactions, N_R, the total number of active species, N, and the stoichiometric matrix, $\boldsymbol{A}$, which captures the interactions among all species within the network. Furthermore, the CRN must adhere to linear algebra constraints such that $N_R \leq N$ [15] because there cannot exist more independent reactions than active species. Using this information, we can derive an optimisation problem of which the solution details the mass balance of species, $\boldsymbol{S}$, as a function of net reactions, $\boldsymbol{R}$, across N_e experiments. The formulation used, given a single experiment n, is shown in Equation 3

$$\begin{aligned} \frac{dS_1}{dt} &= \sum_{i=1}^{N_R} \alpha_{1,i} r_i \\ &\vdots \\ \frac{dS_N}{dt} &= \sum_{i=1}^{N_R} \alpha_{N,i} r_i \end{aligned} \tag{3}$$

where $\alpha_{N,i}$ is the stoichiometric coefficient for an individual species within net reaction, i.

Once the reaction rates are determined, it is imperative to ensure they are independent from one another. Many techniques exist to this purpose; however, we employ the use of sparse optimisation such that we can simultaneously minimise the total number of identified net reactions and find the corresponding rate profiles. The methodology for this procedure is outlined in Figure 2.

In order to find the minimum dimension reaction network that well fits experimental data, we conduct parameter estimation using the modified least squares objective function in Equation 4, subject to mass and atomic balance constraints.

$$\min_{\boldsymbol{R}(t),\boldsymbol{A}} \sum_{n=1}^{N_e} (\boldsymbol{S}_n - \boldsymbol{S'}_n(\boldsymbol{R}(t),\boldsymbol{A}))^2 + \lambda \sum_{i=1}^{N_R} \sum_{j=1}^{N} \frac{\alpha_{j,i}}{\alpha_{j,i} + \epsilon} \tag{4}$$

Here $\boldsymbol{S}$ and $\boldsymbol{S'}$ are the measured and simulated species concentrations, λ is a weighting parameter, and the term $\frac{\alpha_{j,i}}{\alpha_{j,i}+\epsilon}$ encourages model sparsity by minimising the rank of the stoichiometric matrix.

Reaction Rate Model Generation

Once the global reaction rates have been identified, a SR based approach is implemented to automatically generate representative reaction rate equations directly from the estimated rate profiles, using available literature to exclude terms with no physical relevance to the system under study. We overcome the limitation of SR for complex systems by introducing a substructure decomposition strategy that breaks down the global reaction rates into various terms, each with physical meaning (e.g., forward and reverse reaction rates), as shown in Figure 3.

As illustrated in Figure 3, after the initial candidate expression has been suggested by SR, the individual substructures are then iteratively updated and fine tuned and, once this local iteration completes, MBDoE is performed by maximising the variance between the predictions of the pareto front of SR candidate functions.

RESULTS AND DISCUSSION

Results of the Methanol Synthesis Reaction Network

As described in the case study section, the methanol synthesis via CO_2 reaction network consists of 6 species in a closed system, meaning that there is a maximum of 5 global reactions. By deriving the problem formulation in Equation 3 and using the sparse optimisation methodology in Figure 2 and Equation 4 to solve the parameter estimation framework, we obtain a set of independent reaction rates, $\boldsymbol{R}$, and stoichiometric coefficients, $\boldsymbol{A}$. Upon rescaling the values of the stoichiometric coefficients to ensure they are all of integer values, we are left with the reduced reaction network in Equation 5

$$\begin{aligned}
\frac{dF_{CO}}{d\tau} &= r_2 \\
\frac{dF_{CO_2}}{d\tau} &= -r_1 - r_2 - r_3 \\
\frac{dF_{H_2}}{d\tau} &= -3r_1 - r_2 - 4r_3 \\
\frac{dF_{CH_3OH}}{d\tau} &= r_1 \\
\frac{dF_{H_2O}}{d\tau} &= r_1 + r_2 + 2r_3 \\
\frac{dF_{CH_4}}{d\tau} &= r_3
\end{aligned} \tag{5}$$

where F_j is the molar flow rate of species j and τ is the residence time.

When equated to the ground truth in reaction network R1, it can be seen that they are identical. The use of mass and atomic balance constraints allowed for side reactions with minimal influence to be discovered, as is true of the Sabatier reaction, r_3, which holds reaction rates 10-100 times less that of r_1 and r_2.

With the establishment of a valid reaction network, the second stage of the workflow can proceed, enabling the creation of reaction rate models from data. As symbolic regression leverages genetic algorithms to design candidate expressions, it is necessary to introduce approaches to reduce the search space that must be explored to improve solution quality. This can be achieved in several manners, namely the use of structural constraints and imposing restrictions on the list of operators, $\boldsymbol{\varphi} = \{+, -, \times, \div, x_a\}$, and inputs. Within the literature surrounding heterogenous catalysis, it is commonplace to use Langmuir-Hinshelwood type structures to define the kinetics present and, as such, we can enforce SR to abide by the structural form as shown Equation 6.

$$r_i = \frac{f_i(\boldsymbol{S}, \theta) - g_i(\boldsymbol{S}, \theta)}{(1 + h_i(\boldsymbol{S}, \theta))^n} \tag{6}$$

In this manner, the proposed equations will be more interpretable, and we can decompose the LH models based on their definition, where the numerator relates to the thermodynamic driving force and the denominator represents the kinetic resistance. A further advantage stems from stage 1 of the workflow. Since a complete reaction network has been attained, the input features can be curated based on these results, as we have knowledge of which species participate within each reaction, including within the different substructures (forward rate, reverse rate and kinetic inhibition).

Following the iterative SR procedure outlined in Figure 3, 8 further experiments were designed and incorporated into the algorithm, with the best performing models of the final iteration listed in Table 1.

Table 1: Top ranked discovered Langmuir-Hinshelwood type equations from the iterative SR procedure in Figure 3. $a_{j,i}$ is a parameter of model i.

Rate	Equation
r_1	$\frac{\alpha_{1,1}P_{CO_2}P_{H_2}^2 - \alpha_{1,2}P_{CH_3OH}P_{H_2O}}{P_{H_2}(1 + \alpha_{1,3}P_{CO_2}P_{H_2} + \alpha_{1,4}P_{H_2} + \alpha_{1,5}P_{CO_2} + \alpha_{1,6}P_{CO_2}^2)}$
r_2	$\frac{\alpha_{2,1}P_{CO_2}P_{H_2} - \alpha_{2,2}P_{CO}P_{H_2O}}{(\alpha_{2,3} + \alpha_{2,4}P_{CO_2} + \alpha_{2,5}P_{H_2})(\alpha_{2,6} + \alpha_{2,7}P_{CO_2} + \alpha_{2,8}P_{H_2})}$
r_3	$\frac{\alpha_{3,1}P_{H_2}(1 - \frac{\alpha_{3,2}P_{CH_4}P_{H_2O}^2}{P_{H_3}^3})}{(\alpha_{3,3} + \alpha_{3,4}P_{CO_2} + \alpha_{3,5}P_{H_2})(\alpha_{3,6} + \alpha_{3,7}P_{CO_2} + \alpha_{3,8}P_{H_2})}$

From an analysis of Table 1, there exists considerable equivalence to the ground truth structures in Equation 1, indicating that the methodology was capable of learning crucial insight from the data regarding the kinetics. Specifically, the algorithm discerned that, not only do H_2 and CO_2 individually affect the kinetic resistance, but their interactions also have a substantial contribution. Additionally, in the methanol synthesis (r_1) and water gas shift reactions (r_2), the influence of CO_2 the on the forward rate and CH_3OH, CO, and H_2O on the reverse rates were correctly identified as first order. Although, for r_1, the order of P_{H_2} was determined to be 2 instead of 3, the dominant impact of H_2 in the forward reaction rate was uncovered correctly.

As well as providing deep insight into the kinetics of the reaction, the parameterisation of the models in Table 1 yielded low average fitting percentage errors of 3.3% as shown in Figure 4. In order to assess the predictive capabilities across the entire design space, an experiment was designed to discriminate between the generated SR models and the ground truth. The maximum

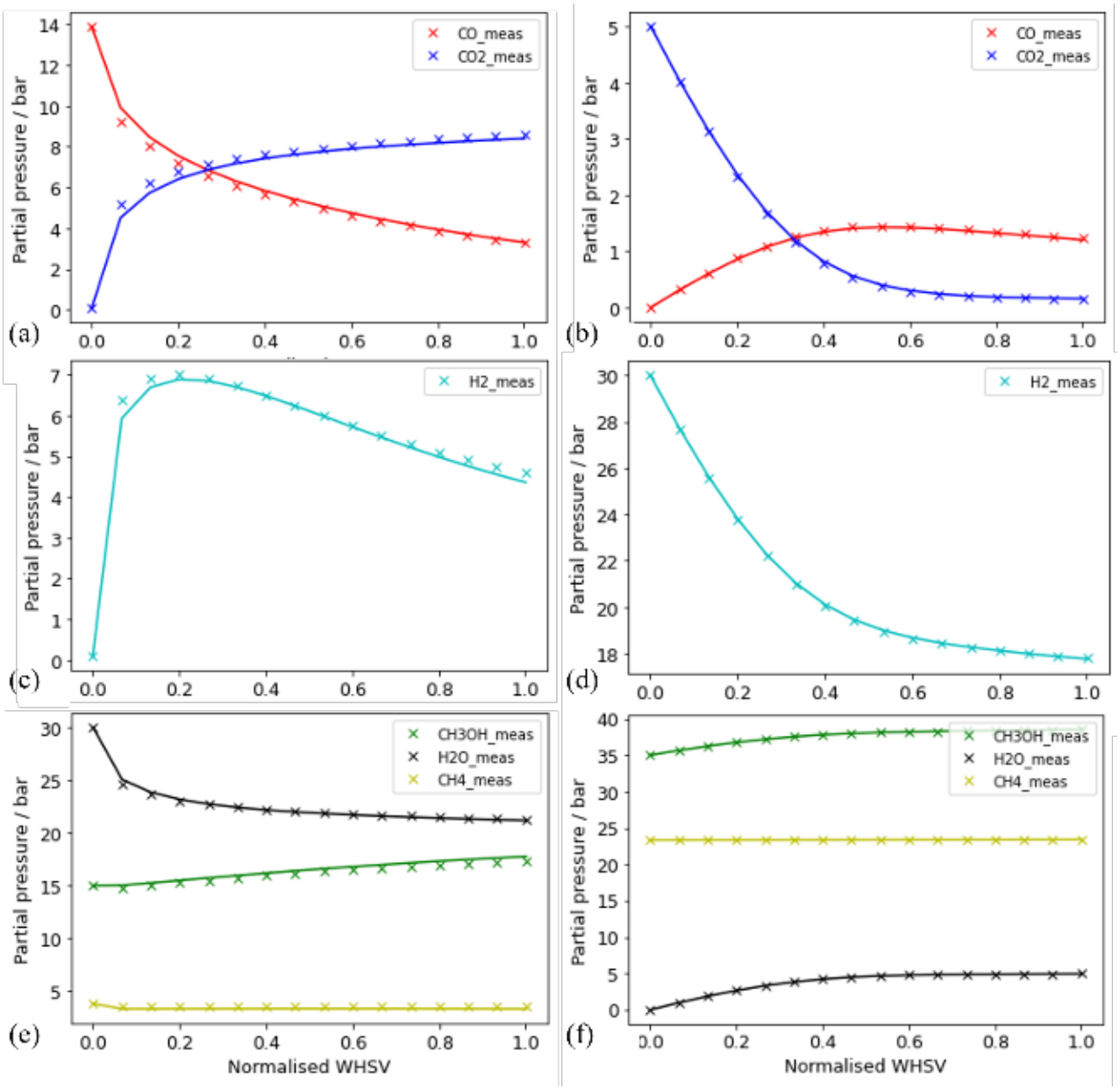

Figure 4. Fitting results of the top ranked SR generated models on the MBDoE experiments. (a), (c), and (e) refer to a single experiment and (b), (d), and (f) to another.

average percentage error across the entire operational region was 16.9%, demonstrating that the framework is robust and data efficient, being able to capture highly complex underlying kinetic information with a limited experimental budget.

Results of the Kinetic Resolution Network

In a similar manner to the methanol synthesis reaction network, we can derive the problem formulation in Equation 3 using 9 active species and therefore a maximum of 8 independent reactions. After solving the problem formulation, it was discovered that only 5 global reactions are required to fit the experimental data, with the final reaction network presented in Equation 7.

$$
\begin{aligned}
r_1&\colon\ VA \rightleftharpoons \mathrm{AE} + AA \\
r_2&\colon\ AE + S_1 \rightarrow S_2 \\
r_3&\colon\ VA + S_2 \rightarrow AA + S_3 \\
r_4&\colon\ AE + R_1 \rightarrow R_2 \\
r_5&\colon\ AE + R_2 \rightarrow R_3
\end{aligned}
\tag{7}
$$

Through comparing the results in Equation 7 to the ground truth (R2), it is possible to observe that all the

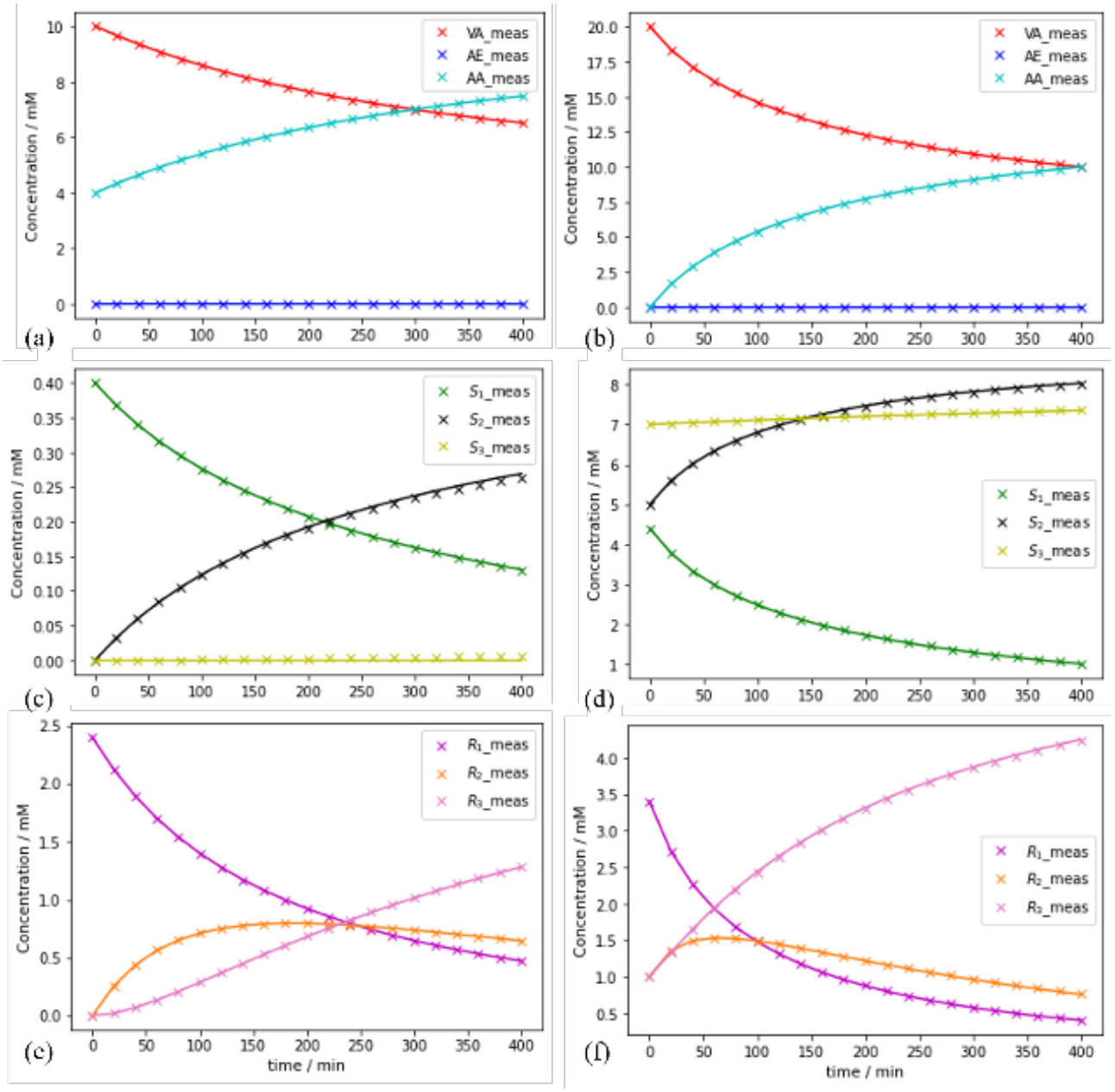

Figure 5. Fitting results for the parameterised SR models in Table 2. (a), (c), and (e) refer to a single experiment and (b), (d), and (f) to another.

species that are involved within the reactions as well as their respective stoichiometric coefficients were found with the sole inconsistency being in r_3, where VA and AA were included in place of AE. Notably, this is a lumped representation of the r_1 and r_3 in the ground truth reactions and still satisfies all mass balances. Therefore, the result is physically valid. It is hypothesised that the lumped representation was found due to the high dimensional nature of the optimisation problem requiring over 240 parameters to be solved for. This issue is further complicated by the low relative magnitudes of reaction rates for r_3 being 10-1000 times smaller than the reaction rates of all other reactions.

The accurate determination of four global reaction rates provides affirmation of the accuracy and reliability of the developed methodology. Applying the parameterised reaction network in Equation 7 to the initial 4 experiments used for network identification yields minimal percentage errors ($\approx 0\%$), both proving the effectiveness of the strategy, yet also a limitation where recovered reactions may, in actuality, be a lumped representation of the several ground truth reactions.

With the construction of a suitable reaction network, SR can now be applied as dictated in Figure 3. Similar to the previous case study, the literature can be exploited to add suitable constraints to the inputs, operators $\varphi = \{+, -, \times, \div, x_a\}$ and the equations structure. Succeeding the first iteration of running the framework, it was surmised that no further MBDoE was needed due to the correct rate models being recovered immediately for all reactions except r_3, as shown in Table 2, with a fitting percentage error of 3.0%.

Table 2: Top ranked rate models discovered for the kinetic resolution case study.

Rate	Equation
r_1	$\alpha_{1,1}C_{VA} - \alpha_{1,2}C_{AA}C_{AE}$
r_2	$\alpha_{2,1}C_{S_1}C_{AE}$
r_3	$\alpha_{3,1}C_{S_3}C_{VA}$
r_4	$\alpha_{4,1}C_{R_1}C_{AE}$
r_5	$\alpha_{5,1}C_{R_2}C_{AE}$

From Table 2, the interpretability of the generated model structures is apparent, indicating first order dependencies with respect to any species involved, and that all reaction rates possess irreversible behaviour apart from r_1. Finally, in both case studies, none of the proposed reaction rate models exhibited complexities beyond that of the ground truth kinetics, providing strong evidence that the framework is capable of yielding highly interpretable and precise representations that describe the underlying reaction networks.

CONCLUSION

The case studies presented demonstrate that the proposed two-stage framework is capable of accurately recovering underlying reaction networks and automatically constructing interpretable kinetic rate expressions consistent with known physics, operating effectively under a limited experimental budget. Furthermore, the novel iterative application of symbolic regression mitigates the risk overly complex model forms, increasing the practical applicability of SR to real-world reaction systems whilst preserving high levels of interpretability.

Importantly however, the present study is conducted assuming complete observability of all reacting species and noise-free measurements, which are rarely fully satisfied in industrial practice. Future research should therefore assess the robustness of the framework when applied to noisy and sparsely sampled experimental datasets. Nevertheless, when combined with human-in-the-loop guidance, the methodology shows considerable promise for gaining mechanistic insight to support expert analysis. By incorporating augmented intelligence within the workflow, the framework offers a pathway towards accelerated knowledge generation and automated kinetic modelling for complex reaction engineering applications.

REFERENCES

1. Becker C. From langmuir to ertl: the “nobel” history of the surface science approach to heterogeneous catalysis. Encyclopedia of Interfacial Chemistry :99-106 (2018). https://doi.org/10.1016/b978-0-12-409547-2.13527-9
2. Marin GB, Yablonsky GS, Constales D. Kinetics of chemical reactions. Wiley (2018). https://doi.org/10.1002/9783527808397
3. Motagamwala AH, Dumesic JA. Microkinetic modeling: a tool for rational catalyst design. Chem. Rev. 121:1049-1076 (2020). https://doi.org/10.1021/acs.chemrev.0c00394
4. Nakajima EA, Oliveira LG, Gasparrini LJ, Souza GEQ, Ignacio AA, Alves HJ, Borba CE. Kinetics of dry reforming of methane catalyzed by ni/si-mcm-41. International Journal of Hydrogen Energy 48:32331-32341 (2023). https://doi.org/10.1016/j.ijhydene.2023.05.010
5. Armenise, S.; García-Bordejé, E.; Valverde, J.; Romeo, E.; Monzón, A. A Langmuir–Hinshelwood approach to the kinetic modelling of catalytic ammonia decomposition in an integral reactor. Phys.
6. Ali SH. Kinetics of catalytic esterification of propionic acid with different alcohols over amberlyst 15. Int J of Chemical Kinetics 41:432-448 (2009). https://doi.org/10.1002/kin.20416
7. Mendoza-Covarrubias C, Romero CE, Hernandez-Rosales F, Agarwal H. N₂o formation in selective non-catalytic no_x reduction processes. JEP 02:1095-1100 (2011). https://doi.org/10.4236/jep.2011.28126
8. FISHTIK I, DATTA R. A NEW APPROACH FOR THE CLASSIFICATION AND ENUMERATION OF UNIQUE REACTION ROUTES AND UNIQUE OVERALL REACTIONS IN MULTIPLE CHEMICAL REACTION SYSTEMS. Chemical Engineering Communications 191:373-397 (2004). https://doi.org/10.1080/00986440490272555
9. Miskovic L, Béal J, Moret M, Hatzimanikatis V. Uncertainty reduction in biochemical kinetic models: enforcing desired model properties. PLoS Comput Biol 15:e1007242 (2019).

https://doi.org/10.1371/journal.pcbi.1007242
10. Taylor CJ, Seki H, Dannheim FM, Willis MJ, Clemens G, Taylor BA, Chamberlain TW, Bourne RA. An automated computational approach to kinetic model discrimination and parameter estimation. React. Chem. Eng. 6:1404-1411 (2021). https://doi.org/10.1039/d1re00098e
11. Taylor CJ, Booth M, Manson JA, Willis MJ, Clemens G, Taylor BA, Chamberlain TW, Bourne RA. Rapid, automated determination of reaction models and kinetic parameters. Chemical Engineering Journal 413:127017 (2021). https://doi.org/10.1016/j.cej.2020.127017
12. Ghosh S, Sebastian J, Olsson L, Creaser D. Experimental and kinetic modeling studies of methanol synthesis from CO2 hydrogenation using in2o3 catalyst. Chemical Engineering Journal 416:129120 (2021). https://doi.org/10.1016/j.cej.2021.129120
13. Gustavo MF, Székely E, Tóth J. Kinetic modeling of a consecutive enzyme-catalyzed enantioselective reaction in supercritical media. ACS Omega 5:26795-26806 (2020). https://doi.org/10.1021/acsomega.0c02405
14. Dong J, Zhong J. Recent advances in symbolic regression. ACM Comput. Surv. 57:1-37 (2025). https://doi.org/10.1145/3735634
15. Feinberg M. Species-reaction graph foundations. Applied Mathematical Sciences :419-440 (2019). https://doi.org/10.1007/978-3-030-03858-8_19